

**ENHANCEMENT OF MUNICIPAL WASTEWATER BIOSOLIDS DRYING
THROUGH INTERFACIAL ENERGY MODIFYING AMENDMENTS TO
PROMOTE UNIFORM AGGLOMERATION**

by

HELIN ZHANG

A Thesis

Submitted to the Faculty

of the

WORCESTER POLYTECHNIC INSTITUTE

In partial fulfillment of the requirements for the

Degree of Master of Science

in

Environmental Engineering

by

July 2018

APPROVED:

Professor John Bergendahl, Ph.D., Advisor

Professor Jeanine D. Plummer, Ph.D., Committee Member

ACKNOWLEDGEMENTS

I wish to thank all the following people who gave me incredible help for my thesis, without their help, it would not have been possible.

I would like to especially thank my advisor Professor John Bergendahl for his expertise and excellent cooperation. And for all the opportunities I was given to conduct my research. You provided me with the tools that I needed to choose the right direction and successfully complete my thesis.

I would like to thank all staffs in Civil and Environmental Engineering department involved with the analyses, they support me a lot with their generous help. I also would like to thank Gericke's lab for providing the laboratory facilities and supplies to conduct this research.

Additionally, I would like to thank CARD (Center for Advanced Research in Drying) for sponsoring my research.

TABLE OF CONTENTS

ACKNOWLEDGEMENTS	i
LIST OF TABLES	iii
LIST OF FIGURES	iv
ABSTRACT.....	v
INTRODUCTION AND BACKGROUND	1
MATERIALS AND METHODS	17
Sample Collection and Preparation.....	17
Scanning electron microscopy (SEM) Analysis	18
Inductively coupled plasma – mass spectrometry (ICP-MS) Analysis.....	19
Dynamic light scattering (DLS) Analysis	20
Zeta potential measurements	21
Surface properties modifications trials	22
Particle Sizes Changes with Amendments at Optimal Dose	23
RESULTS AND DISCUSSIONS	24
SEM Images	24
ICP-MS Analysis	26
Zeta-potential Measurements	28
Surface Properties Modification Trials.....	32
Particle sizes changes with amendments at optimal dose	38
SUMMARY AND FUTURE WORK.....	42
REFERENCES.....	45
APPENDIX.....	49

LIST OF TABLES

Table 1 Typical Chemical Composition of Untreated Primary and Activated Sludge..	2
Table 2 Typical Metal Content of Biosolids	3
Table 3 Metals Concentrations in Biosolids	26
Table 4 Conversion of Electrical Conductivity to Ionic Strength.....	29
Table 5 Properties and structures for studied polyelectrolytes	33

LIST OF FIGURES

Fig. 1. Drying process flow diagram of NEFCO facility.....	5
Fig. 2 Diagram of typical rotary dryer (Adapted from Delele <i>et al.</i> , 2015).....	9
Fig. 3 Polymer bridging mechanism.....	13
Fig. 4 Polymer charge neutralization mechanism.....	14
Fig. 5 Polymer electrostatic patch mechanism	15
Fig. 6 The Experimental Design	18
Fig. 7 SEM Micrographs at Different Magnifications	25
Fig. 8 Metals Concentrations in Biosolids.....	错误!未定义书签。
Fig. 9 Zeta-potentials at Ionic Strengths of 0.001 M, 0.01M and 0.1M	29
Fig. 10 Illustration of electrical double layer	31
Fig. 11 Effects of the polyelectrolytes dosage on the zeta-potential.	34
Fig. 12 Comparison of the biosolids particle sizes.	39

ABSTRACT

Large quantities of biosolids are produced from treatment of municipal wastewater and can be processed into a nutrient and organic-rich soil amendment that has great value for agriculture. The drying process involves converting solids at approximately 25-30% solids content to a dry, stable biosolids pellet. The majority of the input material is recycled to the mixing step upstream of the dryer to achieve a more uniform particle size distribution. The objective of this work was to investigate use of polyelectrolyte amendments to promote uniformity in dried biosolids pellet size. Biosolids samples were collected at the New England Fertilizer Company (NEFCO) facility located in Quincy, MA, U.S. The biosolids samples were characterized by scanning electron microscopy (SEM), inductively coupled plasma/mass spectrometry (ICP-MS), dynamic light scattering (DLS) and zeta potential measurements. Five polyelectrolytes, polyethyleneimine (PEI), polydiallyldimethyl-ammonium chloride (PDADMAC), polyallylamine (PAM), polyacrylic acid (PAA) and polyethylene oxide (PEO) were selected as candidate amendments for surface properties modification trials. The results indicated that three cationic polyelectrolytes, PDADMAC, PEI and PAM, reduced the (absolute value) zeta potentials of the biosolids surfaces to near zero. The optimal doses for reducing the zeta potentials were found to be 0.008 mg PEI/mg solids; 0.005 mg PAM/mg solids and 0.03 mg PDADMAC/mg solids, respectively. The anionic polyelectrolyte PAA and nonionic polymer PEO were found to be ineffective for modifying the zeta potential of the biosolids. The changes in particle size distributions of the biosolids using the three cationic polyelectrolytes were determined by dynamic

light scattering (DLS) measurements. Of the three cationic polyelectrolytes, only PDADMAC was found to increase the biosolids particle size from average size of 340 nm to 3600 nm with 240 min contact time. This indicates the potential for PDADMAC as an amendment for improving the biosolids drying process as it was able to decrease the number of fines and increase the “green” biosolids pellet size.

INTRODUCTION AND BACKGROUND

Biosolids are nutrient-rich organic materials resulting from the treatment of domestic wastewater in a treatment facility (U.S. EPA, 2000). In general, biosolids contains about 90 percent water of the total weight and 10 percent of suspended solids consisting of both inorganic mineral and organic portions (WEF/U.S. EPA, 1997). The chemical composition of biosolids may vary considerably between wastewater treatment plants as well as within each treatment plant at different points within the system. Typical data on the chemical composition of wastewater biosolids are reported in Table 1. Concentrations of heavy metals associated with the biosolids may vary widely, as indicated in Table 2. Chemical constituents including nutrients can be seen as the significant factor in the ultimate disposition of the processed sludge and processes related to water removing processes. Factors that can frequently affect anaerobic digestion process are the values of pH, alkalinity, and organic acid content. Determination of the content of heavy metals, pesticides, and hydrocarbons are in necessary when incineration and land application methods are considered (Metcalf & Eddy, 2003).

Except for the biosolids source, prior treatment for biosolids can also affect particle sizes of the biosolids. The largest particle size achieved at primary clarifier since fine suspended and colloidal solids passing quickly through it, resulting in the primary biosolids containing more of inorganic and fibrous materials than secondary biosolids

and activated biosolids. During biological treatment, the removal of primary biosolids are accomplished along with the creation of the less dense, flocculated cellular material. Most of dissolved BOD has been removed during the activated sludge process by bio-coagulation and flocculation, hence the activated sludge biosolids is created, which is consequently the finest among primary biosolids and secondary biosolids. Typically, these biosolids is made up of more than 60–90% cellular organic material and a large amount of water (Wang *et al.*, 2007).

Table 1 Typical Chemical Composition of Untreated Primary and Activated Sludge Biosolids (Adapted, in part, from EPA, 1979)

Item	Untreated		Untreated	
	Primary Sludge		Activated Sludge	
	Range	Typical	Range	Typical
Total dry solids (TS), %	1-6	3	0.4-1.2	0.8
Volatile solids (% of TS)	60-85	75	60-85	70
Grease and fats (% of TS)	5-8	6	5-12	8
Protein (% of TS)	20-30	25	32-41	36
Nitrogen (N, % of TS)	1.5-4	2.5	2.4-5	3.8
Phosphorous (P ₂ O ₅ , % of TS)	0.8-2.8	1.6	2.8-11	5.5
Cellulose (% of TS)	8-15	10	-	-
Iron (not as a sulfide)	2-4	2.5	-	-
Silica (SiO ₂ , % of TS)	15-20	-	-	-
pH	5-8	6	6.5-8	7.1
Alkalinity (mg/L as CaCO ₃)	500-1500	600	580-1100	790
Organic acids (mg/L as HAc)	200-2000	500	1100-1700	1350
Energy content, kJ/kg VSS	23,000-29,000	25,000	19,000-23,000	20,000

Table 2 Typical Metals Content of Biosolids (EPA, 2009)

Metal	Range of dry solids, mg/kg
Arsenic	1.18-49.2
Cadmium	0.21-11.8
Chromium	6.74-1160
Cobalt	0.87-290
Copper	115-2580
Iron	1575-299,000
Lead	5.81-450
Manganese	34.8-14,900
Mercury	0.17-8.3
Molybdenum	2.51-132
Nickel	7.44-526
Selenium	1.1-24.7
Tin	7.5-522
Zinc	216-8550

About 7,100,000 dry tons of biosolids are generated each year among approximately 16,500 municipal wastewater treatment facilities in the U.S. (U.S. EPA, 2004). Through the drying process which will be discussed in the later section, a relatively dry, soil-like material, can be produced by separating the solids from the wastewater. After thermally removing additional water from the mechanically dewatered cake, biosolids product is produced.

The input material to the dryer typically has less-than-ideal uniformity, which results in finer sized material passing quickly through the dryer, and larger sized material is held up in the dryer with greater residence times. The majority of the material is recycled to the mixing step upstream to the dryer to achieve a better uniformity of particle size. This research focused on using polyelectrolyte amendments to promote uniformity in biosolids pellet size to reduce energy consumption for drying municipal wastewater biosolids.

Researchers point out that in attempting to convert “waste” biosolids to beneficial use is the addition of biosolids to soil, which is called land application, in order to supply nutrients and replenish soil organic matter. Approximately more than a half of the total biosolids generated each year are land applied, the residual biosolids are for the applications like incineration, composting and landfill (NEBRA, 2007). Land application of biosolids have been wide spread as an effective method throughout the United States, Canada and Europe for more than 40 years. Many studies have demonstrated the positive effect of land application of sewage sludge or sludge compost on corn and forage yields and soils (Warman, 1986; Tiffany *et al.*, 2000 and Zorpas, 2012). Biosolids can also be used on agricultural land, forests, rangelands, or on disturbed land in need of reclamation (U.S. EPA, 2000; Vasileski, 2007). However, land application, according to Zorpas (2008), is considered to be one of the most important disposal alternatives.

Biosolids land application has some disadvantages, i.e., it can be labor intensive, cause odor concern by the public and have negative impacts to soil due to mismanagement. However, if the stringent record keeping and reporting requirements on both the federal and state level are imposed to prevent mismanagement, in that case, the biosolids land application programs may be properly managed and have beneficial use (U.S. EPA, 2000).

Recycling biosolids through land application serves several purposes: it improves soil properties, supplies nutrients essential for plant growth and serves as an alternative or substitute for expensive chemical fertilizers. The nutrients in the biosolids consist mostly of organic materials which has a slower release to growing plants compared to chemical inorganic fertilizers. Inorganic fertilizers are more likely to leach into groundwater or run off into surface water due to the higher water solubility of them (U.S. EPA, 2000).

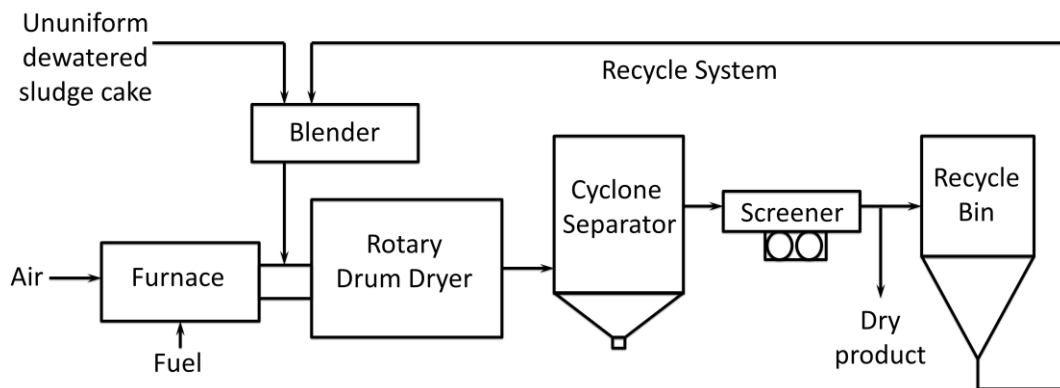


Fig. 1. Drying process flow diagram of NEFCO facility.

Biosolids samples were collected at the New England Fertilizer Company (NEFCO) drying facility located in Quincy, MA, U.S. The anaerobically digested sludge is transferred from the Massachusetts Water Resources Authority (MWRA) Deer Island Treatment Plant (DITP) to NEFCO through dual sludge pipelines. Sludge transfer takes place 4 to 5 days per week with an average of 2 million gallons per day pumped. Direct heat from gas fired furnaces is used for treating and processing the residuals sludge. The Biosolids Processing Facility (BPF) utilizes dryer process trains to transform sludge. The processing system at NEFCO Quincy consists of six process trains with three trains typically running simultaneously. Each train can process 6,500 dry pounds of sludge per hour. Mixing of sludge and dewatering polymer is completed at the storage tanks. The blend is then pumped to two centrifuges through one process train for dewatering. Fig. 1 demonstrates the drying process flow diagram of the NEFCO facility. The dewatered sludge cake (with about 25-30% solids) is mixed in pug mills with previously dried fines collected from the biosolids screens downstream to the dryers. The blend of cake and fines is conveyed by the biosolids process trains to the triple-pass rotary drum dryers. A cyclone separator is used for separating the discharged dried pellet biosolids and unqualified biosolids from the air stream. The unqualified biosolids are conveyed to the recycle system for a better size distribution and the dry biosolids products, are screened and collected. Only 1 percent of the final product is bagged for local distribution by MWRA; the rest of the products is shipped to customers in bulk through land transportation. The distribution for the land application of the bulk

product is listed as follows: agricultural uses (40-50%), fertilizer blending (30-35%), and as an alternative fuel (20-30%).

According to Metcalf & Eddy (2003), there are three categories for heat dryers: direct, indirect, combined direct-indirect, and infrared. The most frequently used dryers for municipal biosolids drying are direct and indirect dryers. Other methods (coal, oil, gas, infrared radiation, or dried sludge) may serve as an energy supplement for heat drying.

As discussed by Metcalf & Eddy (2003), there are three commonly used direct drying technologies involved in drying of municipal wastewater sludges and biosolids, which are the flash dryer, rotary dryer, and fluidized-bed dryer. The demand for flash dryers has been continuously decreasing in the United States due to safety concerns, high energy requirements, high O&M, and limited interest from vendors to work in the wastewater market (WEF, 2010). Considering that fluidized-bed drying is a relatively new application in the United States, rotary dryers are currently the most common dryers for wastewater sludges or biosolids (Fagernäs *et al.*, 2010, Pang and Mujumdar, 2010).

Recently, rotary dryers, a form of direct dryer, have been used widely for the drying of waste activated sludge, raw primary sludge and digested biosolids. The mechanism for the fundamental heat transfer of direct dryers is convection, exposed the product

directly contacting with the drying medium (hot air) (Delele *et al.*, 2015). Metcalf & Eddy (2003) pointed out rotary dryers are made up of a cylindrical steel shell that is rotating on bearings around its axis at a low slope as shown in Fig. 2.

Lifting flights are implicated in most types of rotary dryers. The product is lifted by the flights and released at certain height; the solids then fall as “dispersed” material (Fig. 2) during shell rotation. The separated solid material falls through the flowing high temperature, dry air (Delele *et al.*, 2015). The flow of the material is assisted by the lifting flights along with the increase contact area between the high temperature air and the drying material. “The mixture of dewatered sludge and hot gases are conveyed to the discharge end of the dryer. During conveyance, axial flights along the rotating interior wall pick up and cascade the sludge through the dryer” (Metcalf & Eddy, 2003). Researchers noticed that the majority of the drying happens during this product-cascading period (Bacelos *et al.*, 2009, Fernandes *et al.*, 2009 and Lisboa *et al.*, 2007). Industrial rotary dryers typically have a vessel shell with dimensions in the range of 0.3-3 m, 1.2-30 m, and 0-4° in diameter, length, and inclination, respectively. The shell typically rotates at 4-8 rpm, with a temperature of 121-288°C of dry air, and air mass velocity in the rotary dryers is in the range of 0.5-5 kg/s·m² (Mujumdar, 2004 and Moyer *et al.*, 1997).

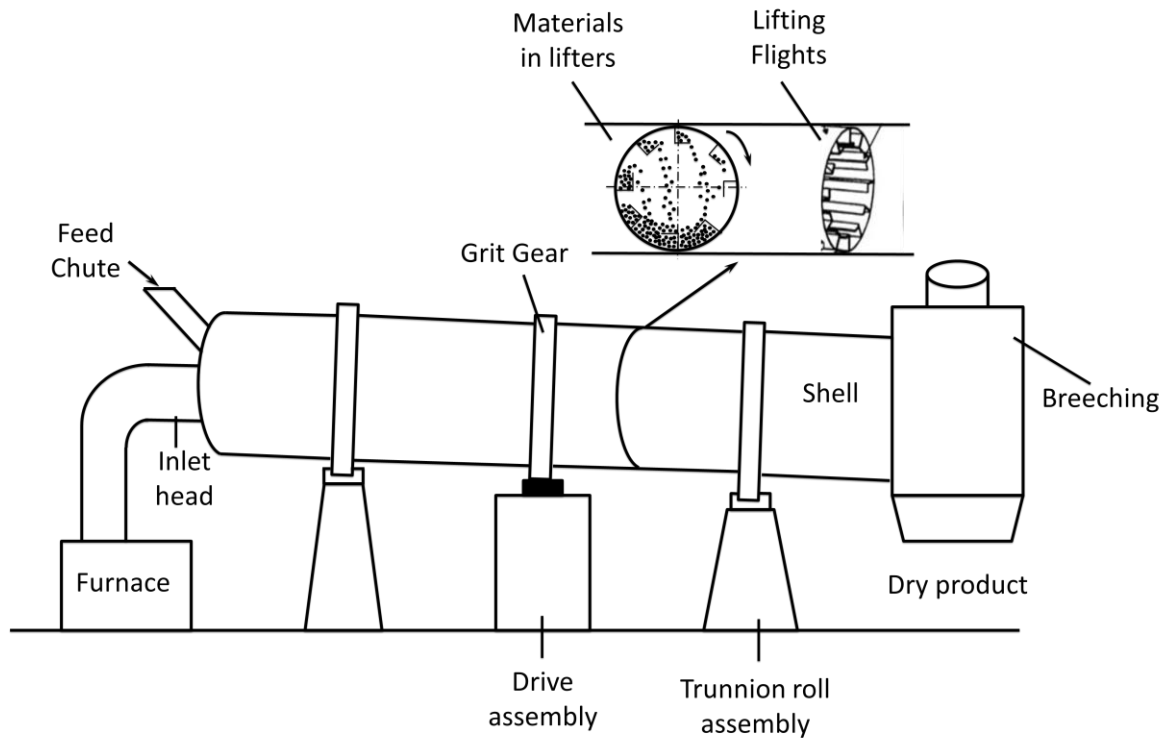


Fig. 2 Diagram of typical rotary dryer (Adapted from Delele *et al.*, 2015)

In convection (direct drying) systems, wet sludge or biosolids are contacted directly with the heat transfer medium, usually hot gases. WEF (2010) emphasized the concept that: “under equilibrium conditions of constant rate drying, mass transfer is proportional to (1) the area of wetted surface exposed, (2) the difference between water content of the drying air and saturation humidity at the wet-bulb temperature of the solid-air interface, and (3) other factors, such as velocity and turbulence of drying air expressed as a mass transfer coefficient”. The heat-transfer rate for evaporation is determined by the following equation:

$$q_{conv} = h_c \cdot A(T_g - T_s)$$

Where q_{conv} = convective heat transfer rate, kJ/h (Btu/h)

h_c = convection heat transfer coefficient, $\text{kJ/m}^2 \cdot \text{h} \cdot ^\circ\text{C}$ ($\text{Btu/ft}^2 \cdot \text{h} \cdot ^\circ\text{F}$)

A = area of the heated surface, m^2 (ft^2)

T_g = gas temperature, $^\circ\text{C}$ ($^\circ\text{F}$)

T_s = temperature at sludge/gas interface, $^\circ\text{C}$ ($^\circ\text{F}$)

At the NEFCO Quincy facility, direct heat from gas fired furnaces is used for the treatment and processing of the residuals sludge with 25 million BTU per hour “low NOx” burners.

The dewatering process has been demonstrated to be an effective process before the utilization of thermal drying due to the intense use of energy in drying process. Conditioners are usually added to the digested sludge to generate large flocs which are easy to filter prior to sludge dewatering. Polyelectrolytes, Fe (III), Fe (II), lime, and Al (III) are the most commonly used chemicals for conditioning the sludge. Those chemicals act as “either coagulants by reducing the zeta potential of the solid particles or flocculants through the bridging effect to form proper-sized flocs” (Chen *et al.*, 2002).

In this study, the approach of using polymers to enhance biosolids agglomeration is expected to capitalize on the similar mechanism of using polymers to improve the conditioning during the dewatering process. Although the biosolids have different moisture content compared to the dewatered sludge cake, the difference between the effects of drying and dewatering driven by polyelectrolytes is expected to be negligible.

Also, information on the use of the polyelectrolytes amendments for the drying process is extremely lacking in the literature. For this reason, this study focused on the investigation of using polyelectrolytes to promote more uniform pellet size with less dry recycle material. The degree of agglomeration can be assessed from the change of particle size or floc size. The results of this study are compared to the results of polymer amendments for dewatered sludge during dewatering process due to the lack of data for drying.

According to Bratby (2006), polyelectrolytes consist of a large variety of natural or synthetic, water-soluble, macromolecular compounds. They may cause destabilization and improvement of flocculation of particulate constituents in water. Soluble organic polymers can be divided into three categories: nonionic polymers, anionic polymers, and cationic polymers. The manufacturing and application of soluble polymers for use in wastewater sludge treatment has been significantly improved in recent times. Polymers are now universally applied in the sludge conditioning process (Wang *et al.*, 2007). Various anionic, cationic and nonionic polyelectrolytes have been used to modify surface energetics of materials in wastewater treatment and will be explored as amendments for this application.

As has been discussed by Bratby (2006), the mechanism of destabilization by polyelectrolytes can be ascribed to two principal mechanisms, “which in some instances may operate conjointly, whereas in others, the predominance of one over the other is fairly simple to identify. In some cases, the two phenomena may operate in opposition”. The first mechanism is called the bridging mechanism. It refers to the binding of polyelectrolytes and colloid particle surfaces as the polymer portions are adsorbed on the surfaces of adjacent colloids, thereby providing a “bridge”. The other mechanism is due to charge neutralization. The potential energy of repulsion between adjacent colloids is reduced by the adsorption of ionic polyelectrolytes to the opposite charged suspended materials. These two theories of destabilization, charge neutralization and interparticle bridging, can both have great influence on conventional polymer conditioning for biosolids.

It has been well accepted that the bridging mechanism (Fig. 3) is operative in flocculation by polymers since mid-19th century (Healy and La Mer, 1962; Michaels, 1954; Ruehrwein and Ward, 1952). “The stages in the bridging mechanism are dispersion of polyelectrolyte in the suspension, adsorption at the solid-liquid interface, compression or settling down of the adsorbed polyelectrolyte and collision of adjacent polyelectrolyte-coated particles to form bridges and thereby increasingly larger flocs”. Each of these stages is discussed in detail elsewhere (Bratby, 2006).

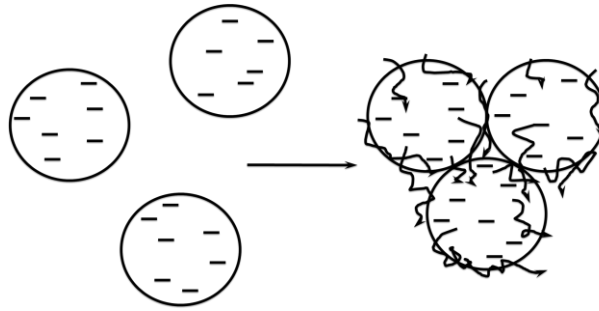


Fig. 3 Polymer bridging mechanism

It is essential for effective bridging flocculation that there should be enough uncoated surface on a given particle for attachment of segments of polymer chains adsorbed on other particles. In order to avoid insufficient bridging, an optimum dosage of polymer to give the most effective flocculation is necessary (Gregory, 2006).

In addition to polymer bridging, there is another important mechanism that can be very useful in conditioning process: charge neutralization as shown in Fig. 4. Particles in wastewaters are typically negatively charged. Cationic polyelectrolytes are often found to be the most efficient flocculants, which can preferentially adsorb on negatively charged particles. In this application, the cationic polyelectrolytes are considered to be primary coagulants or flocculants. The mixing intensity is an important factor that affects charge neutralization; only the proper amount of mixing intensity will be able to bring about the adsorption of the polymer onto the colloidal particles due to the large number of particles in wastewater. Metcalf and Eddy (2003) also emphasized that without adequate mixing, the effectiveness of the polymer will be diminished. Further,

if the number of colloidal particles is limited, it will be difficult to remove them with low polyelectrolyte dosages.

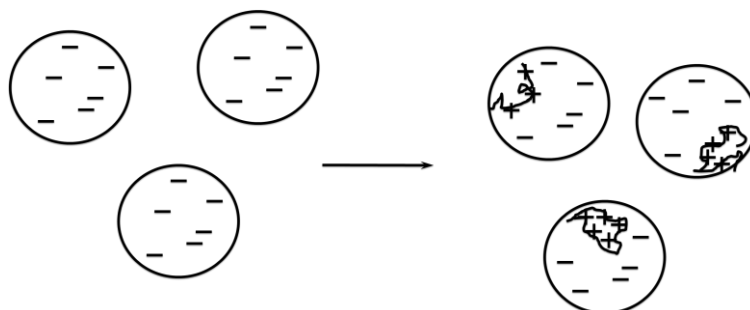


Fig. 4 Polymer charge neutralization mechanism

The exclusivity of the bridging mechanism was examined by Kasper (1971) and Gregory (1973). The electrostatic patch mechanism has been proposed for systems where strong electrostatic attraction between the polyelectrolyte and particle surface exists (as shown in Fig. 5). The electrostatic patch theory was first introduced by Gregory (1973) to explain the coagulation of low charge density particles with oppositely charged polymers of very high charge density. As Gregory (2006) has discussed, “when highly charged cationic polyelectrolytes adsorb on particles with a fairly low negative surface charge density, it is not physically possible for each surface charge to be individually neutralized by a cationic segment of the adsorbed chain. The average distance between charged surface sites may be significantly lower than the spacing between cationic sites on the polymer chain. So, although overall charge neutralization may occur, at a suitable polymer dosage there will be a local

heterogeneity of charge, giving a charge mosaic or electrostatic patch arrangement”, shown schematically in Fig. 5.

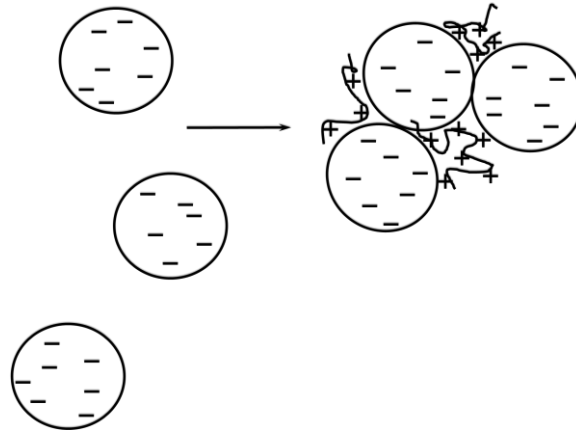


Fig. 5 Polymer electrostatic patch mechanism

Mohammad *et al.* (2016) claimed that laboratory experiments indicated that cationic polymer managed to reduce the charge of the zeta potential values; however, the anionic polymers were not effective in causing any neutralization. Ayol *et al.* (2005) investigated the single and dual polymer conditioning of water treatment residuals. Results showed that using a cationic polymer produced a less turbid supernatant. Zeta potential and streaming current were not good indicators of conditioning efficacy when a nonionic polymer was used, and the implementation of dual polymer use does not appear warranted, although some studies indicated that dual polymer can improve dewaterability (Chitikela and Dentel, 1998; Fan *et al.*, 2000; Lee and Liu 2000, 2001).

It is hypothesized that polyelectrolytes amendments that modify the interfacial energy of the biosolids will provide for controlled, more uniform agglomeration. It is expected that more uniform pellet size will allow reduction in dryer air flow and dryer combustion energy consumption, and produce a more valuable, consistently-sized, biosolids product. Thereby, the following objectives were developed:

- Characterization of wastewater treatment biosolids properties;
- Identify amendments based on potential for modifying interfacial energy to promote uniform agglomeration;
- Evaluate amendments for modifying surface energy properties of biosolids, and
- Evaluate uniformity of biosolids pellet size with the addition of select amendments.

MATERIALS AND METHODS

Sample Collection and Preparation

In this study, the digested dewatered sludge cake was collected in two 1L containers (Sho-me, U.S.) to maintain *in-situ* moisture contents and delivered to the laboratory within 2 hours. Samples were transferred into clean glass jars that were capped after sample collection and stored at 4°C. The solids content as collected was approximately 25%. Samples were then dried in evaporating dishes at 105°C for 24 hours in a laboratory oven. The samples were gently crushed into powders with a mortar and pestle and stored in reagent tubes (Corning, U.S.) in a desiccator until use. All sample containers and apparatus were cleaned with soap water, rinsed with purified water, and dried before use. Purified water was produced with a Thermo Scientific Barnstead Nanopure Life Science UV/UF system with a TOC analyzer (effluent TOC < 5 µg/L).

The methodology was divided into three parts which are: biosolids characterization, surface properties modification trials and particle sizes changes with amendments at optimal dose. An overall experimental design and components of each phase are shown in Fig. 6.

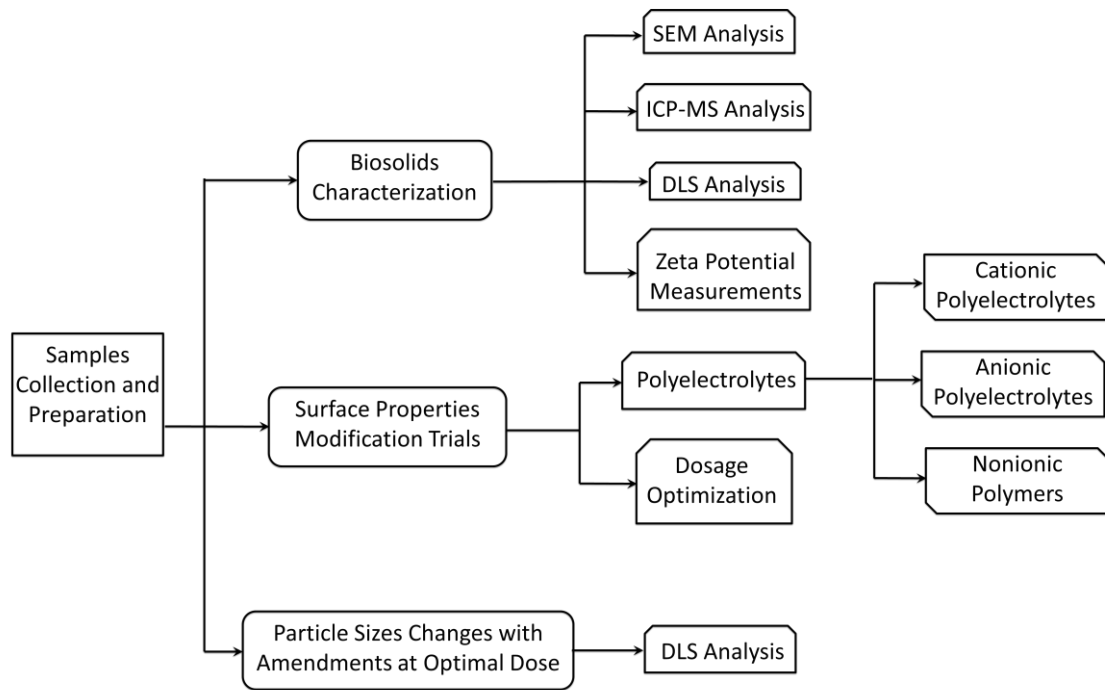


Fig. 6 The Experimental Design

Scanning Electron Microscopy (SEM) Analysis

SEM produces images of a sample by scanning the surface with a focused beam of electrons. The surface topography and composition of the sample can be obtained by producing various signals that related to the interaction with electrons and atoms. The position of the secondary electron beam which works in a raster scan pattern is connected with the detected signal to produce an image. The specimens can be observed at resolutions smaller than 1 nanometer under high vacuum (Stokes, 2008).

Samples were compressed into a wafer and mounted using double-sided conductive tape. Surface dust above the samples was removed by blowing a compressed gas. The

SEM used was a JSM-7000F from JEOL (USA). The instrument settings were: accelerating voltage = 3 kV, probe current at 3×10^{-11} A, and working distance (WD) = 15 mm. Imaging was conducted magnifications ranging from 35 to 20,000 X.

Inductively Coupled Plasma – Mass Spectrometry (ICP-MS) Analysis

Inductively Coupled Plasma Mass Spectrometry is a multi-element analysis technique for detecting metals and several non-metals at concentrations as low as one part in 10^{15} (part per quadrillion), using inductively coupled plasma as an ion source and a mass spectrometer as its detector. According to the ICP-MS manual from PerkinElmer (2016), before the sample test, the instrument was warmed up for half an hour and a standard performance check was run to ensure proper resolution, mass calibration, sensitivity and stability of the ICP-MS. The sampling tubes and the samplers were rinsed in between every sample.

The targeted isotopes were Al-27, V-51, Cr-52, Mn-55, Fe-57, Co-59, Ni-61, Cu-63, Zn-66, As-75, Cd-111 and Pb-208. ICP-MS can detect the signal intensity for the given atomic number elements. For samples preparation, 0.5 grams of each sample were transferred to 100 ml beakers, followed by acidification with 2.5 ml concentrated HNO_3 (Fisher Chemical, 60-70% purity). After digesting for 24 hours, filtration was carried out using glass or plastic funnels fitted with filter paper (Whatman, Catalog No.

1004110). Purified water was added to the supernatant to bring the sample volumes back to 50 ml in reagent tubes (Corning Centristar, U.S.) for further measurements. The samples were analyzed with a NexION 350X from PerkinElmer.

Dynamic Light Scattering (DLS) Analysis

DLS has been well applied to analyze submicron particles as a general technique which has the ability to measure particles with sizes less than one nanometer. The characterization of particles is one of the typical applications of DLS analysis, which have been dispersed in a liquid. Malvern (2004) indicated that “the small particles are constantly moving due to Brownian motion, which is the thermal movement of particles due to the random collision with the molecules of the liquid that surrounds the particle. Brownian motion causes laser light to be scattered at different intensities. Analysis of these intensity fluctuations yields the velocity of the Brownian motion and hence the particle size using the Stokes-Einstein relationship”.

$$d(H) = \frac{kT}{3\pi\eta D} \quad \text{Equ.1}$$

Where $d(H)$ = hydrodynamic diameter

D = translational diffusion coefficient

k = Boltzmann's constant

T = absolute temperature

η = viscosity

The determination of the rate of the intensity fluctuation can be measured by the Zetasizer Nano system which can use this result to calculate the size of the particles (Malvern, 2004).

For sample preparation, three 0.1 g samples were transferred into 200 mL beakers with 100 ml purified water, then subjected to an ultrasonic bath (Branson 1510) for 15 minutes. After the disposable cell was cleaned with purified water, the sample was transferred to the cell. Dynamic light scattering measurements were taken with a Zetasizer Nano ZS by Malvern.

Zeta Potential Measurements

The evaluation of particle stability and the effectiveness of flocculation can be accomplished by measuring the zeta potential at the surface of solid sludge particles (Mohammad *et al.*, 2016). The zeta potential of biosolids was measured using Zetasizer Nano ZS by Malvern. The migration of the particles in suspension is driven by an electric field which causes particles to move toward one of the electrodes. The direction of migration is affected by the charge of the surface potential of the particles (positive or negative charge), and the magnitude of the surface potential has an important influence on the velocity which the zeta potential and electrophoretic mobility can be

investigated. The zeta-potential is the potential (in mV) at the double layer plane of shear by separating the mobile from the fixed double layer (Bergendahl, 2017).

For sample preparation, three 0.1 g samples were transferred into 200 mL beakers with 100 ml purified water in each. This provided a solution of 1000 mg/L of biosolids. The solutions were subjected to an ultrasonic bath for 15 minutes to disperse the solids. The zeta potentials of three replicate samples were measured at pH values varying from 2 to 10. The zeta potential for one solution was measured without adding any NaCl. Predetermined masses of NaCl (Fisher Scientific, $\geq 99\%$) were added to the other two solutions to bring ionic strength from the original ionic strength of the solution (approximately 0.001 M) up to 0.01 M and 0.1 M. The zeta potentials were determined at varying pHs (from 2 to 10) by Malvern Zetasizer Nano ZS. The instrument operational procedure was according to the Zetasizer Nano user manual (2004).

Surface Properties Modifications Trials

The polyelectrolytes that were trialed in these experiments include cationic PEI (Sigma-Aldrich, USA), cationic PDADMAC (Sigma-Aldrich, USA), cationic PAM (Polysciences, Inc., USA), anionic PAA (Polysciences, Inc., USA) and nonionic PEO (Thermo Fisher, Inc., USA). As the zeta potential measurements indicated surfaces with negative potentials, the cationic amendments were expected to partially “neutralize” the

surface potential, attenuating the electrostatic repulsion. This should allow favorable aggregation of the biosolid fines. The general approach was to dose the biosolids with prescribed amounts of polyelectrolyte and evaluate (measure) the zeta potential changes with the Zetasizer. The optimal dosage of each polyelectrolyte was recorded while the zeta potential is close to zero.

The predetermined volume of each polyelectrolyte solution was transferred by a pipette to the biosolids solution in a 200 mL capacity beaker. The mixed materials were fixed on a magnetic stirring apparatus with Teflon-coated stir bar at 400 rpm at room temperature. After a mixing period of approximately 15 to 20 minutes, the solutions became ready for use. Procedures for zeta potential measurement (in the former section) was followed to determine the effect of the polyelectrolytes on zeta potential.

Particle Sizes Changes with Amendments at Optimal Dose

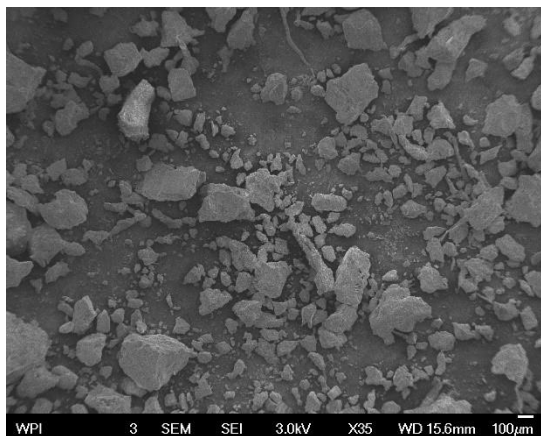
Three cationic polyelectrolyte solutions (at optimal dose determined from surface properties modification trials) were added into the biosolid solution. The solutions were mixed on magnetic stirring apparatuses with Teflon-coated stir bars at 100 rpm at room temperature. The particle sizes were measured by Malvern Zetasizer Nano ZS with increasing contact time (up to 4 hr), with time increments of approximately 1 hr.

RESULTS AND DISCUSSIONS

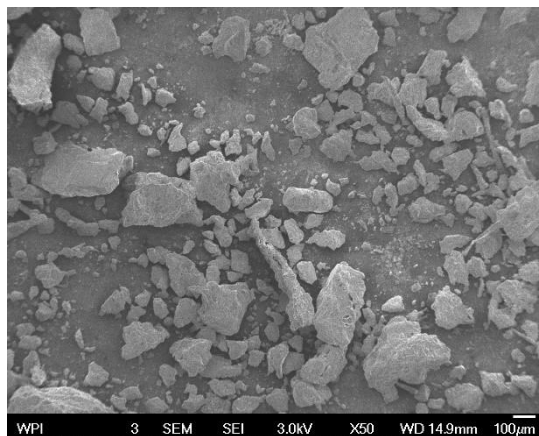
SEM Images

SEM micrographs of the external surface of dried samples of biosolids at magnifications of 35x to 20000x are shown in Figs. 7a-f. At magnifications greater than 20,000x, image focusing was not successful.

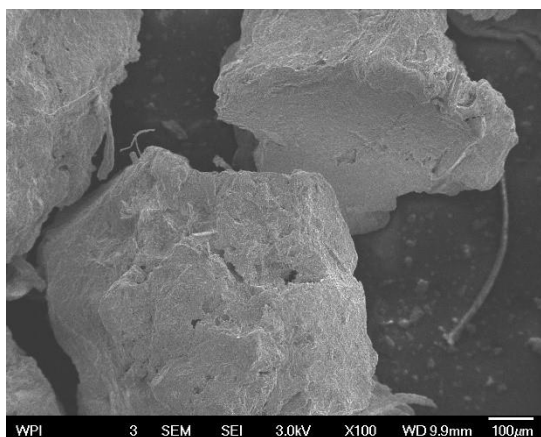
Observations at low magnification allow examining the whole structure. At low magnification (Figs. 7a-c), the structure of the biosolids samples appear dense and compact. The dried biosolids floc size is approximately between 10 μm to 500 μm . At higher magnification (Figs. 7d-f), the structure of biosolids samples appear to be made of a complex arrangement of dried bacteria and other elements aggregated. The surface of samples presents rather smooth, with some surface cracks apparent. Flocculated cellular material is created during biological treatment, and it is expected that the structure and topography of the biosolids samples would be strongly dependent on the drying process. And, biosolids particle size become smaller and denser with greater shear/grinding time. According to Wang *et al.* (2007), both the biosolids source and prior treatment can have influences on the final biosolids particle size. With flocculation, the particular bio particles of anaerobically digested sludge are usually aggregated to a certain extent. Different biosolids (different origin and/or different processes) may exhibit different surface characterization that are difficult to predict *a priori*.



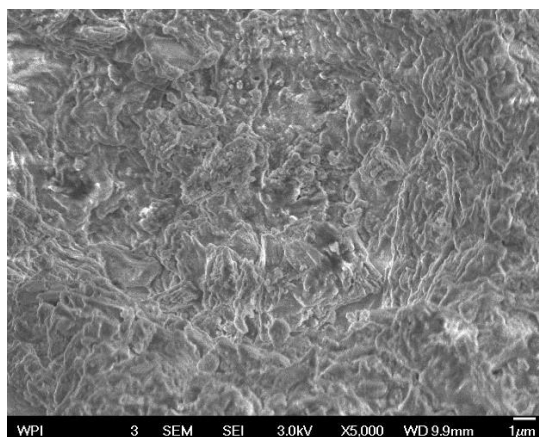
(a)



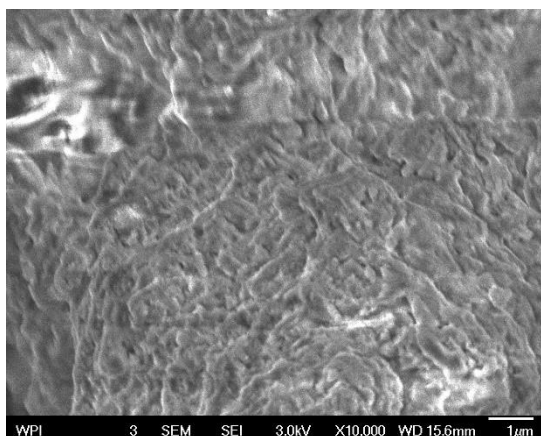
(b)



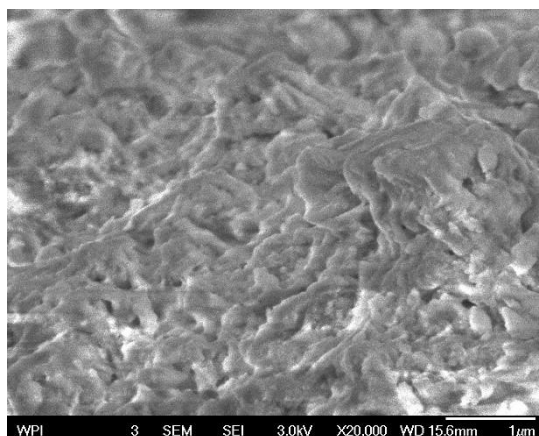
(c)



(d)



(e)



(f)

Fig. 7 SEM Micrographs at Different Magnifications (a) 35X; (b) 50X; (c) 100X; (d) 5,000X; (e) 10,000X; (f) 20,000X.

ICP-MS Analysis

Samples were collected from the NEFCO Quincy facility, and ICP-MS analysis conducted for elements of interest. The concentrations of select elements are listed in Table 3.

Table 3 Metals Concentrations in Biosolids (average shown; error bars indicate 95% confidence interval (CI))

Pollutant	Average Pollutant Concentration (mg/kg)	Pollutant Concentration Limits (U.S. EPA 1993, and 1994) (mg/kg)
Aluminum (Al)	$6.682 \cdot 10^3$	NL
Vanadium (V)	22.41	NL
Chromium (Cr)	73.92	NL
Manganese (Mn)	$5.338 \cdot 10^2$	NL
Iron (Fe)	$5.009 \cdot 10^4$	NL
Cobalt (Co)	13.89	NL
Nickel (Ni)	51.88	420
Cu (Copper)	$6.035 \cdot 10^2$	1500
Zn (Zinc)	$1.160 \cdot 10^3$	2800
As (Arsenic)	15.30	41
Cd (Cadmium)	13.66	39
Pb (Lead)	$1.240 \cdot 10^2$	300

Note: NL = No limit

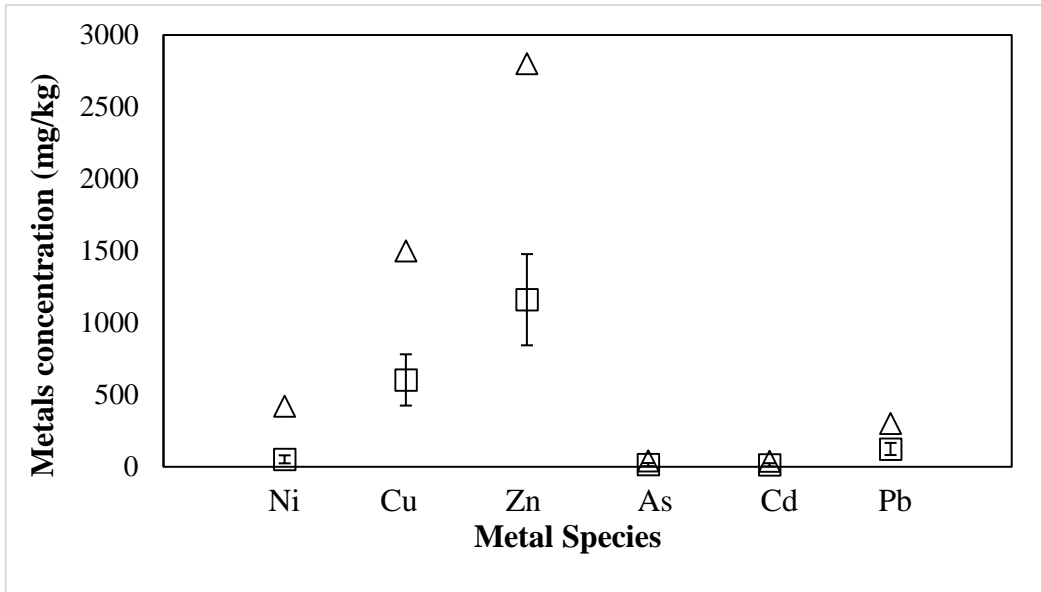


Fig. 8 Metals Concentrations in Biosolids (black triangles represent pollutant concentration limits and black squares represent average pollutant concentrations of triplicate samples, error bars indicate 95% CI)

Biosolids samples were collected from the NEFCO drying facility (Quincy, MA). In general, except for the elements that are not limited by U.S. EPA, the intensities of other elements (Fig. 8) are all comparatively lower than their pollutant concentration limits. This indicates that the biosolids samples have the potential to be a Class A biosolids product which can be used as a high-end fertilizer for agriculture.

Jacobs (2001) pointed out that components of arsenic, cadmium, copper, mercury, molybdenum, nickel, selenium and zinc are of most concern due to their toxicity to plant, animal or human. among the pollutants in biosolids. Other metals commonly present in biosolids are manganese, iron, lead, aluminum and chromium. Except for cadmium, these elements are not expected to have any significant harm to human

consumers but can supply nutrients to soil for crop growth and production. This can be contributed to the low solubility of those elements in soil and the small amount of these metals in biosolids that their addition to soils can be negligible. In addition, according to Chaney and Ryan (1993), compounds such as ferric hydrous oxides, organic matter and phosphate can lower the bioavailability of these nutrients to plants, animals and humans by binding pollutants to the biosolids.

The concentration of iron found in the samples (41,702 mg/kg) is greater than the concentrations of the other elements; aluminum (5724.8 mg/kg) was present in lower concentration than iron. One possible reason for the presence of iron and aluminum at such high concentrations may be due to their use for enhancing sedimentation or clarification.

Zeta-potential Measurements

Zeta-potential (ζ) of biosolids samples were measured under varying pH and ionic strengths in order to characterize the biosolids surface chemistry. In this work, ionic strengths of the sample solutions were calculated from measured electrical conductivity (EC) using the following empirical correlation (Snoeyink and Jenkins, 1980) Equation 2, and shown in Table 4.

$$I (\text{mol/L}) = 1.6 \cdot 10^{-5} \cdot \text{EC}(\mu\text{s/cm}) \quad \text{Eq.2}$$

Table 4 Conversion of Electrical Conductivity (EC) to Ionic Strength (I) of biosolids samples solution

EC ($\mu\text{s/cm}$)	Ionic strength (mol/l)
85.7	$1.37 \cdot 10^{-3}$
80.5	$1.30 \cdot 10^{-3}$
80.4	$1.29 \cdot 10^{-3}$

Thus, ionic strength of each sample is shown in Table 4 using equation 2. Higher ionic strength (0.01 M and 0.1 M) samples were obtained by adding NaCl to the solution. Zeta-potential was then determined under a wide pH range with these three different ionic strengths, shown in Fig. 9.

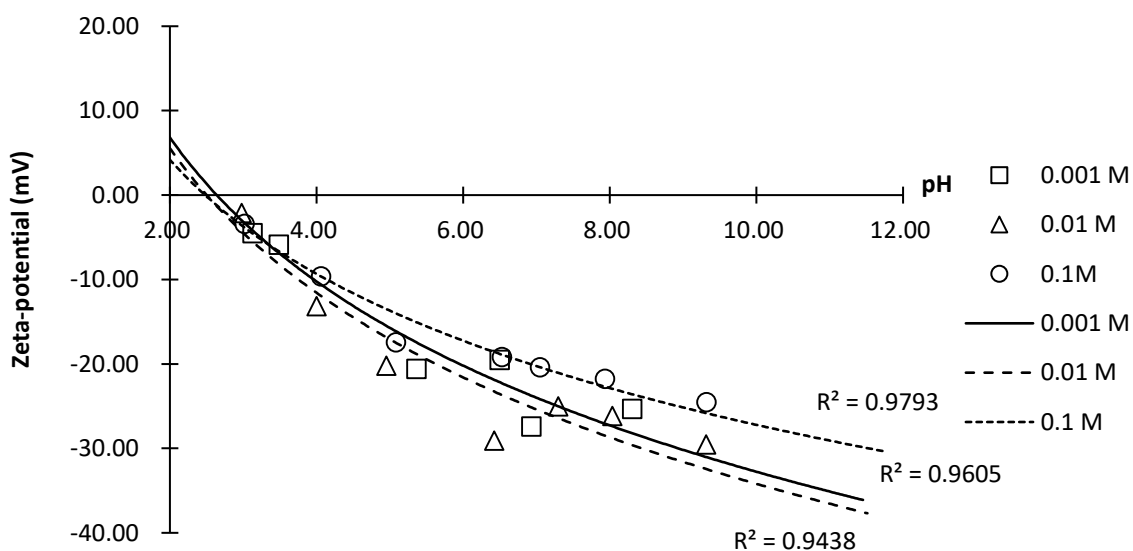


Fig. 9 Zeta-potentials at ionic strengths of 0.001 M, 0.01 M and 0.1 M as a function of pH (Average of triplicates)

Fig. 9 uses logarithmic trendlines fit the zeta potentials data. The coefficient of correlation is represented by the R^2 value: the nearer the value of R^2 to 1, the stronger the correlation of the data (Everitt, 2002). The R^2 values for the fits for ionic strengths 0.001 M, 0.01 M and 0.1 M are 0.9605, 0.9438 and 0.9793, respectively, which indicate a good fit between the data and the three trendlines. As shown in Fig. 9, at low pH (around 2), zeta-potentials at the three different ionic strength are all at the range of positive 5 to 10 millivolts (mV). With increasing pH, the zeta potentials decreased (more negative values) for all ionic strengths. And, at greater pHs, the lower ionic strengths had lower (more negative) zeta potentials.

As indicated by Bratby (2006), many solid surfaces contain functional groups which are readily ionizable. The charge of particles with surfaces with functional groups becomes dependent on the degree of ionization and consequently on the pH of the surrounding liquid. At low pH values, a positively charge surface prevails, while at higher pH a negatively charge surface prevails. At some intermediate pH (the isoelectric point), the charge will be zero. Such phenomenon has been observed in this study. The isoelectric point of the biosolids samples is at approximately pH 3.

As have been discussed by Gregory (2006), if a surface is charged, and directly contacted with a solution of ions, then a characteristic distribution of ions in solution as a function of distance from the surface will be produced. Electrical neutrality of the

solution can be maintained by a charged surface and a corresponding excess of oppositely charged ions. The combination of surface charge and the excess charge in solution constitutes the electrical double layer (Fig. 10). Increasing ionic strength typically has a significant effect on double-layer properties, which leads to reductions in the Stern layer potential and results in the compression of the diffuse layer.

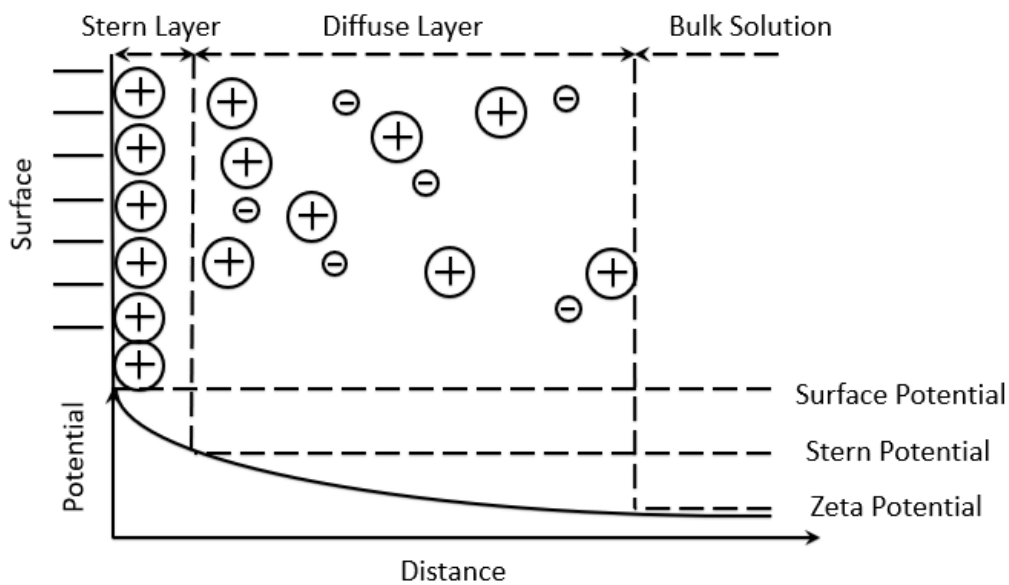


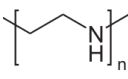
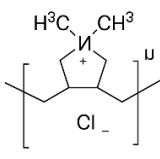
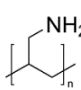
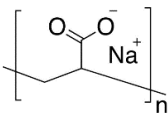
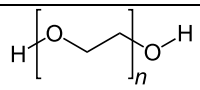
Fig. 10 Illustration of electrical double layer (Adapted from Gregory, 2006).

The zeta potential value increases as the salt concentration increases from 0.01 M to 0.1 M because at higher ionic strength the double layer repulsion is reduced, and a higher zeta potential is needed to maintain stability. Conversely, at low ionic strength (0.001 M), the diffuse layer is larger, and a low zeta potential is sufficient to provide the required repulsion.

Surface Properties Modification Trials

Five polyelectrolytes were selected as candidate amendments for this investigation. Table 5 is a listing of these polyelectrolytes. As the zeta potential measurements indicate surfaces with negative potentials, the cationic amendments are expected to partially “neutralize” the surface potential, attenuating the electrostatic repulsion. This should allow favorable aggregation of the biosolid fines. The general approach was to dose the biosolids with prescribed amounts of polyelectrolyte and evaluate the zeta potential changes.

Table 5 Properties and structures for studied polyelectrolytes

Polyelectrolytes	CAS Number	MW (g/mol)	Structure (repeating unit)	Charging Properties
PEI	9002-98-6	10,000		Cationic
PDADMAC	26062-79-3	200,000-350,000		Cationic
PAM	30551-89-4	15,000		Cationic
PAA	9003-04-7	225,000		Anionic
PEO	25322-68-3	1,000,000		Nonionic

The pH of samples solution is around 6.5 without any pH adjustment. The results for the amendment addition experiments with increasing amendment dosages are shown in Fig.11 below.

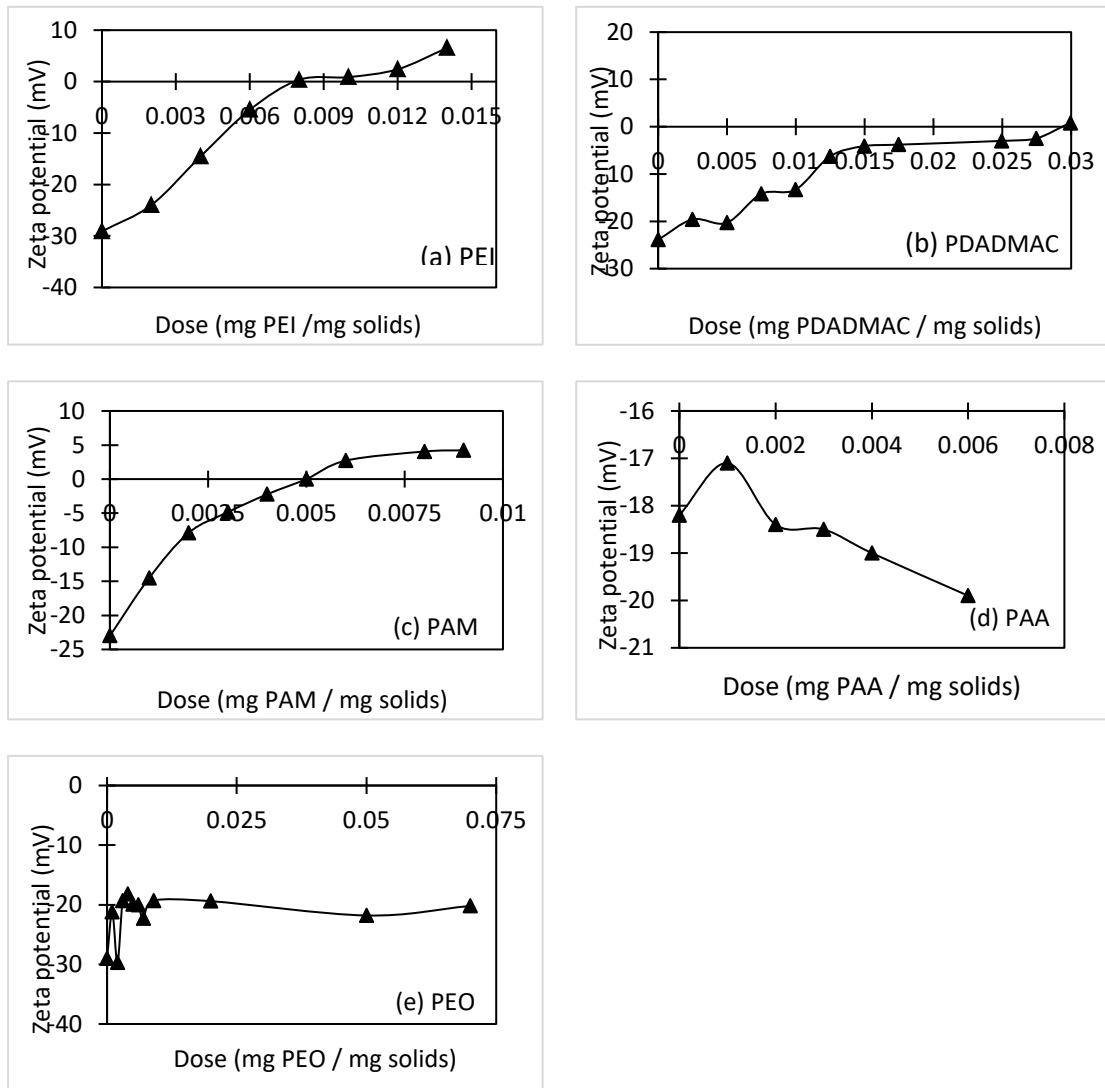


Fig. 11 Effects of the polyelectrolytes dosage on the zeta-potential: (a) PEI; (b) PDADMAC; (c) PAM; (d) PAA; (e) PEO (Single zeta potential measurement at each dose).

The effects of the concentrations of the different polyelectrolytes on the biosolids' zeta potential is shown in Fig. 11. For PEI, the zeta potential of the biosolids particles increases notably as this polyelectrolyte is added. The charge reversal is observed at a polymer concentration larger than 0.008 mg PEI/mg solids. The zeta potential increases with the additional PEI, which indicates that the system is reestablished stabilization.

This phenomenon has also been observed with the addition of two other cationic polyelectrolytes, PDADMAC and PAM. As shown in Fig. 11 (a), (b) and (c), the zeta potentials increase substantially with each incremental addition of polyelectrolyte into the biosolids suspension. All three cationic polyelectrolytes show the ability to reduce the (absolute value) zeta-potential of the biosolids surfaces to near zero, which is the goal of the determination of optimal dose. However, the required dosage of each polyelectrolyte varies, PAM required the lowest dose to reduce the zeta-potential to zero, 0.005 mg PAM/mg solids. The required doses for PEI and PDADMAC were 0.008 and 0.03 mg polyelectrolyte/mg solids, respectively.

Charge neutralization was speculated to be the predominant mechanism of destabilization for the experiments using both PDADMAC and PEI amendments due to their flat configuration adsorption which reduces the likelihood of bridging interactions (Gregory, 2006). This is encouraging as this suggests that the repulsion due to electrostatic repulsion should be significantly reduced, and aggregation of the fines should be promoted. Although PAM has a relatively lower charge density than PDADMAC and PEI, it is likely that charge neutralization plays a more important role than bridging interactions since PAM has a very low molecular weight (15,000 g/mol).

Certain cationic polyelectrolytes have been identified as having the ability to favorably increase aggregation (particle size), as reported by Yu *et al.* (2006). Yu *et al.* found that

the optimal dosage for treating a kaolin suspension by PDADMAC was 0.15 mg/L, which is much lower than the optimal dosage found for treating the biosolids samples in this research.

Fig. 11 (d) showed that the anionic polyelectrolyte PAA did not reduce the zeta potential of the biosolids suspensions. This might be for the following reasons: PAA has low molecular weight, which has been found to be less effective in influencing the size of the molecules in solution and in the adsorbed state. It has generally been found that “linear polymers are more effective than branched or cross-linked structures for a given molecular weight” (Gregory, 2006), which indicates PAA is less effective because of its branched structure.

However, Fan *et al.* (2000), reported that PAA molecules produced large primary flocs that served as the base for adsorption of a second polymer. This reduced the required amount of a second polymer necessary to form binary flocs for their flocculation system. Nevertheless, certain anionic polyelectrolytes show the ability to improve flocculation of primary sludge. These sludge samples were found to have negative zeta potentials (thereby negative surface charge), resulting in anionic polyelectrolytes having no effect on neutralization of the negative charge of the sludge polyelectrolytes.

The ineffectiveness of certain anionic polyelectrolytes was also noted by Mohammad *et al.* (2016). They used the capillary suction time (CST) test for sludge conditioning optimization. The CST test is to determine the rate of water release from sludge. It provides a quantitative measure, reported in seconds, of how readily sludge releases its water. The results were used to assist in the sludge dewatering process and to evaluate sludge conditioning aids and dosages. Higher CST values mean that filtering the sample is more difficult (harder to remove the water). On the other hand, lower CST values indicate that the sample is easier to filter. Their results showed that anionic polymer (Magnafloc LT 27 and Magnafloc LT 25) did not reduce the capillary suction time (CST) values; the increased CST values indicate that the anionic polymer caused the excess polyelectrolytes in sludge sample which make it more difficult to remove water.

Fig. 11 (e) indicated that PEO is ineffective for reducing the zeta potential of biosolids in suspension. Gregory (2006) emphasized the concept that “the effectiveness of polymers as bridging flocculants depends greatly on their properties”. Although PEO has a high molecular weight and a linear structure, the uncharged property indicates that the chains of PEO will not tend to adopt an expanded configuration and only has a small possibility to be effective for biosolids particles bridging.

Interparticle bridging would be expected to be the predominant mechanism for aggregation for most anionic and nonionic polymers. Nonionic polymers are not able

to neutralize the negative charge on the biosolids samples due to their no charge characteristic (Tiravanti, 1985). And anionic polymers also have no effect on the neutralization of the negative charge of the sludge. The low salt concentration of the biosolids suspensions might also have an influence on the failure of bridging action of PAA and PEO. Because low ionic strength would keep chain expansion at a high level and reduce the adsorption on the charged surfaces. In addition, according to Gregory (2006), the flocs produced by polymer bridging which can withstand high shear might be broken and they may not readily reform. The rupture of polymer chains may directly lead to this permanent breakage of flocs, but this aspect is not well understood yet.

In this study, further testing with the anionic polyelectrolyte PAA and nonionic polymer PEO was not carried out. It can be concluded that PAA and PEO do not have any beneficial effect on the destabilization of biosolids particles for this system.

Particle sizes changes with amendments at optimal doses

Particle size distributions were determined by dynamic light scattering (DLS) during aggregation. The DLS results (Fig. 12) are expressed in terms of the peak size which has the largest intensity percentage. DLS analysis indicated the peak size of biosolids macro-colloid particles varied between 200-600 nanometers (nm).

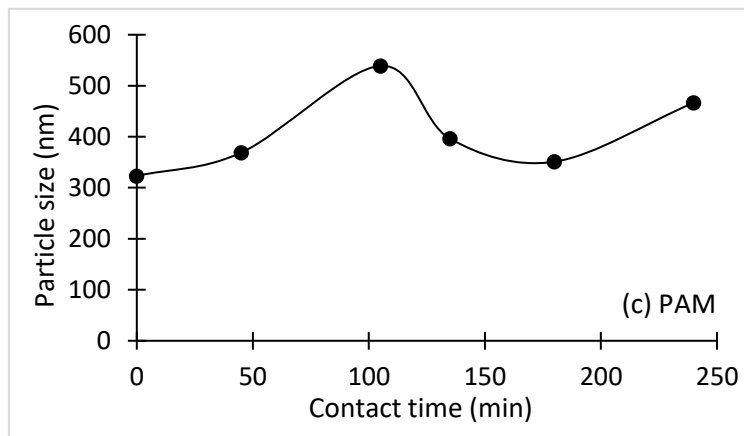
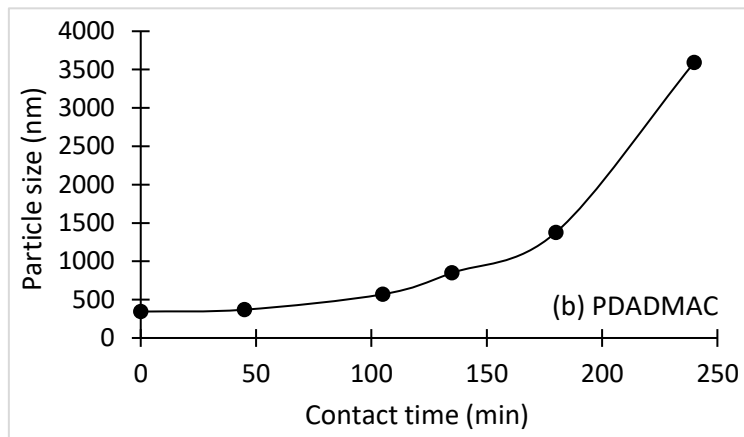
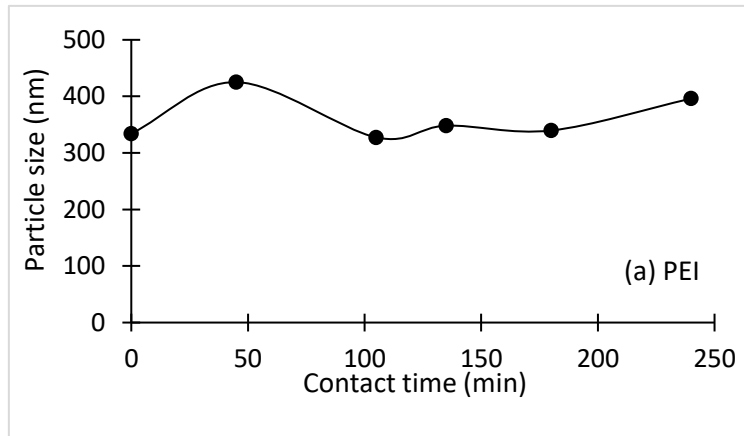


Fig. 12 Comparison of the biosolids particle size by: (a) PEI (0.008 mg PEI/mg solids); (b) PDADMAC (0.03 mg PDADMAC/mg solids); (c) PAM (0.005 mg PAM/mg solids) (data points are average of duplicate experiments).

Fig. 12 demonstrates the particle size of biosolids change with contact time. As the optimal doses of cationic polyelectrolytes (PEI, PAM and PDADMAC) were added to

the samples solution, the biosolids particle size distribution increased with longer contact times (up to 4 hours). The presented data showed that only PDADMAC can improve biosolids particles aggregation with increasing contact time. Unfortunately, PEI and PAM do not show the ability to increase biosolids size distribution.

As shown in Fig. 12 (b), the particle size increases slowly at the initiation of the agglomeration test using PDADMAC. The growth of the agglomerate size reached to its maximum at approximately 240 min using the polyelectrolyte PDADMAC. The floc size was continuously increasing until the end (up to 4 hours) of the flocculation test. At 240 minutes of contact time, the biosolids particle size significantly increased around 700% compared to the initial particle size. The same initial growth tendency was observed in Yu's study, however, when PDADMAC was used in his study, a rapid transformation from relatively low floc size to high floc size was shown within around 12 min; much faster than found in this work.

However, the rapid mixing of two other polyelectrolytes, PEI and PAM, did not significantly alter the particle size until the end of the experiment. For PEI, the largest and smallest particle size during the entire mixing test were 425.2 nm and 327.5 nm respectively. For PAM, the largest and smallest size were 539 nm and 323.2 nm, respectively; which means there was little coagulation and flocculation action driven by PEI and PAM.

The initially slow rates of aggregation with PDADMAC may be explained by its low molecular weight and a large fraction of the added polymer to neutralize the surface charge (Yan *et al.*, 2004). Yu *et al.* (2006) claimed that the highly charged polyelectrolyte PDADMAC tends to adsorb in a flat state. The particle surface and the polyelectrolyte can integrate together in a very short time due to the short chains and small portions of the low molecular weight polyelectrolyte and consequently, the required time for flocculation equilibrium is very short, too. In that case, the probability of interparticle bridging for the adsorbed PDADMAC is less, and interactions between the destabilized particles contact each other directly as a result of the charge neutralization mechanism, which bringing about a slow flocculation rate by PDADMAC (Yu *et al.*, 2006).

SUMMARY AND FUTURE WORK

From SEM micrographs, the sizes of the dried biosolids samples are approximately between 10 μm to 500 μm . At low magnification, the structure of biosolids samples appear dense and compact. At high magnification, the structure of biosolids samples seem made of a complex arrangement of dried bacteria and aggregate-like elements. The surface of samples presents rather smooth and crossed by cracks. SEM micrographs of biosolids samples that have been modified by polyelectrolytes should be considered as a tool for observation during samples aggregation.

From ICP-MS analysis, the concentrations of the elements evaluated in this work are all comparatively lower than their pollutant concentration limits, except for the elements that are not limited by U.S. EPA. This indicates that the biosolids samples have the potential to be a Class A biosolids product which can be used as a high-end soil amendment for agriculture.

Zeta potentials at ionic strengths of 0.001M, 0.01M and 0.1M were determined through a wide range of pH values (2 to 10). At low pH, around 2, zeta-potentials at three different ionic strengths are all at the range of positive 5 to 10 millivolts (mV). At higher pH values, the zeta potentials were increasingly more negative.

Five polyelectrolytes were selected as candidate amendments for surface properties modification trials. Three cationic polyelectrolytes, PDADMAC, PEI and PAM, demonstrate the potential to reduce the (absolute value) of zeta potential to zero. The optimal dose for PDADMAC, PEI and PAM were 0.03, 0.008 and 0.005 mg polyelectrolyte/mg solids, respectively. This is consistent with the charge neutralization mechanism and is encouraging as this suggests that the repulsion due to electrostatic repulsion should be significantly reduced with these amendments – this may translate into modified aggregation performance (less fines, etc.).

The three polyelectrolytes identified as having the ability to favorably adjust the zeta potential of the biosolids were selected for further study for their ability to increase the biosolids particle size. The addition of PDADMAC was able to increase the biosolids particle size significantly with increasing contact time (approximately 700% at 240 minutes of contact time). The other two polyelectrolytes, PEI and PAM, did not alter the particle size.

Future work will entail the development and trial operation of a pilot-scale pug mill system that incorporates an amendment addition sub-system. The “green” biosolids pellet size produced by the system should be measured with the different amendments as a function of time. More samples should be collected over longer times to capture

seasonal impacts, and other amendments for the biosolids samples should also be considered.

REFERENCES

- Ayol, A., Dentel, S. K., & Filibeli, A. Dual Polymer Conditioning of Water Treatment Residuals. *Journal of Environmental Engineering*, **2005**, 131(8), 1132-1138.
- Bacelos, M.; Jesus, D.; Freire, J. Modeling and drying of carton packaging waste in a rotary dryer. *Drying Technology*, **2009**, 27, 927–937.
- Bergendahl, John. Center for Advanced Research in Drying (CARD) Quarterly Report. **2017**.
- Bratby J., *Coagulation and Flocculation in Water and Wastewater Treatment*. London, UK. IWA publishing, **2006**.
- Chaney, R.L., and J.A. Ryan. Heavy metals and toxic organic pollutants in MSW-composts: Research results on phytoavailability, bioavailability, fate, etc. pp. 451-506. In H.A.J. Hoitink and H.M. Keener (eds.), *Science and engineering of composting: Design, environmental, microbiological and utilization aspects*. Renaissance Publications, Worthington, OH, **1993**.
- Chen Guohua, Po Lock Yue & Arun S. Mujumdar, Sludge Dewatering and Drying, *Drying Technology*, **2002**, 20:4-5, 883-916.
- Chitikela, S., and Dentel, S. K. Dual-chemical Conditioning and Dewatering of Anaerobically Digested Biosolids: Laboratory Evaluations. *Water Environ. Res.*, **1998**, 70(5), 1062–1069.
- Delele M. A., F. Weigler & J. Mellmann, Advances in the Application of a Rotary Dryer for Drying of Agricultural Products: A Review, *Drying Technology*, **2015**, 33:5, 541-558.
- Everitt, B., *The Cambridge Dictionary of Statistics*. Cambridge University Press, Cambridge, UK, **2002**.
- Fagnäs, L., Brammer, J., Wilen, C., Lauer, M., Verhoeff, F. Drying of biomass for second generation synfuel production. *Biomass and Bioenergy*, 34, 1267–1277, **2010**.
- Fan, A., Turro, N. J., and Somasundaran, P. “A study of dual polymer flocculation.” *Colloids Surf., A*, **2000**, 162, 141–148.
- Fernandes, N.J.; Ataide, C.H.; Barrozo, A.S. Modeling and experimental study of hydrodynamic and drying characteristics of an industrial rotary dryer. *Brazilian Journal of Chemical Engineering*, **2009**, 26(02), 331–341.
- Gregory J. Rates of flocculation of latex particles by cationic polymers. *J. Colloid Interface Sci.*, **1973**, 42, 2, 448–456.
- Gregory, J. *Particles in Water*. Boca Raton: CRC Press, **2006**.

Healy L.W., La Mer V.K. The adsorption flocculation reactions of a polymer with an aqueous colloidal dispersion. *J. Phys. Chem.*, **1962**, 66, 1835.

Kasper D.R. *Theoretical and experimental investigations of the flocculation of charged particles in aqueous solutions by polyelectrolytes of opposite charge*. Ph.D. Thesis, California Institute of Technology, Pasadena, CA, **1971**.

Lee W. Jacobs and Deliana S. McCreary, Utilizing Biosolids on Agricultural Land. Department of Crop and Soil Sciences, Michigan State University. **2001**.

Lee, C. H., and Liu, J. C. “Enhanced sludge dewaterability by dual polyelectrolytes conditioning.” *Water Res.*, **2000**, 34(18) 4430–4436.

Lee, C. H., and Liu, J. C. “Sludge dewaterability and floc structure in dual polymer conditioning.” *Adv. Environ. Res.*, **2001**, 5, 129–136.

Lisboa, M.H.; Vitorino, D.S.; Delaiba, W.B.; Finzer, J.R.D.; Barrozo, M.A.S. A study of particle motion in rotary dryer. *Brazilian Journal of Chemical Engineering*, **2007**, 24(03), 365–374.

Malvern. Zetasizer Nano Series User Manual, **2004**.

Metcalf & Eddy, Inc. *Wastewater Engineering: Treatment and Reuse*. Boston, USA. McGraw-Hill, **2003**.

Michaels A.S. Aggregation of suspensions by polyelectrolytes. *Ind. Eng. Chem.*, **1954**, 46, 1485.

Moyers, C.G.; Baldwin, G.W. Psychrometry, evaporative cooling, and solids drying. *In Chemical Engineers' Handbook*, 7th ed.; R.H. Perry, D.W. Green, and J.O. Maloney, Ed.; McGraw-Hill: New York, **1997**; Section 12.

Mujumdar, A.S. Dryers for particulate solids, slurries and sheet-form materials. *In Guide to Industrial Drying: Principles, Equipment and New Developments*; A.S. Mujumdar, Ed.; Three S. Colors: Mumbai, **2004**; 37–77.

North East Biosolids and Residuals Association (NEBRA), *A National Biosolids Regulation, Quality, End Use & Disposal Survey* (2007); www.nebiosolids.org.

Pang, S., Mujumdar, A. Drying of woody biomass for bioenergy: Drying technologies and optimization for an integrated bioenergy plant. *Drying Technology*, **2010**, 28, 690–701.

PerkinElmer. ICP-MS Manual. Retrieved April 24, **2016**.

Ruehrwein R.A., Ward D. Mechanism of clay aggregation by polyelectrolytes. *Soil Sci.*, **1952**, 73, 485.

Snoeyink, V.L., and Jenkins, D. *Water Chemistry*, Wiley, New York. **1980**.

Stokes, Debbie J. *Principles and Practice of Variable Pressure Environmental Scanning Electron Microscopy (VP-ESEM)*. Chichester: John Wiley & Sons, **2008**.

Thamer Ahmad Mohammad, Megat Johari Megat Mohd Noor & Abdul Halim Ghazali, Assessment of using synthetic polymers in dewatering of sewage sludge, *Desalination and Water Treatment*, **2016**, 57:48-49, 23308-23317.

Tiffany ME, McDowell LR, O Connor GA, Nguyen H, Martin FG, Wilkinson NS, Cardoso EC. Effects of pasture-applied biosolids on forage and soil concentrations over a grazing season in North Florida. 1. Macro-minerals, crude protein, and in vitro digestibility. *Communications in Soil Science and Plant Analysis*, **2000**, 31, 201-213.

Tiravanti. G, Influence of The Charge Density of Cationic Polyelectrolytes on Sludge Conditioning, *Water Res.*, **1985**, 19(1), 93–97.

U.S. EPA, *Land Application of Biosolids*, Biosolids Technology Fact Sheet, EPA 832-F-00-064, U.S. Environmental Protection Agency, Office of Water Washington, DC, **2000**.

U.S. EPA, *Process Design Manual Sludge Treatment and Disposal*, EPA 625/1-79-011, Office of Research and Development, U.S. Environmental Protection Agency, Washington, DC, **1979**.

U.S. EPA, *Report to Congress on Impacts and Controls of Combined Sewer Overflows and Sanitary Sewer Overflows*, EPA 833-R-04–001, U.S. Environmental Protection Agency, **2004**.

U.S. EPA, *Targeted National Survey-Overview Report*, EPA/822/R-08/014, U.S. Environmental Protection Agency, Washington, DC, **2009**.

Vasileski G, Beneficial uses of municipal wastewater residuals – Biosolids, Canadian Water and Wastewater Association, Final Report, Ottawa, Canada, ,**2007**, pp. 1-26.

Wang L.K., Nazih K. Shammam and Yung Tse Hung. Biosolids Treatment Processes. *Handbook of Environmental Engineering (Vol 6)*, **2007**.

Warman PR, Effects of fertilizer, pig manure, and sewage sludge on timothy and soils. *Journal of Environmental Quality*, **1986**, 15, 95-100.

WEF, *Design of Municipal Wastewater Treatment Plants*, 5th ed., Manual of Practice no. 8, vol. 3, Chaps. 20–27, Water Environment Federation, Alexandria, VA, **2010**.

WEF/U.S. EPA, *Biosolids Fact Sheet Project Biosolids: A Short Explanation and Discussion*, Water Environment Federation and U.S. Environmental Protection Agency, **1997**.

Yan Y.D., S.M. Glover, G.J. Jameson, S. Biggs, The Flocculation Efficiency of Polydisperse Polymer Flocculants, *Int. J. Miner. Process*, **2004**, 73, 161–175.

Yu Jianfeng, Wang Dongsheng, Ge Xiaopeng, Yan Mingquan, Yang Min, Flocculation of kaolin particles by two typical polyelectrolytes: A comparative study on the kinetics and floc structures, *Colloids and Surfaces A: Physicochemical and Engineering Aspects*, **2006**, 290:1–3, 288-294.

Zhao Y.Q., D.H. Bach, Integrated effects of applied pressure, time, and doses on alum sludge dewatering behavior, *Water Manage.* **2007**, 22 (2002) 813–819.

Zorpas A. A., Sewage sludge compost evaluation and utilization. In: Sewage Sludge Management; From the past to our Century, A. A. Zorpas and J. V. Inglezakis (eds), *Nova Science Publishers*, NY, USA, **2012**, pp. 173-216.

Zorpas A. A., Sewage Sludge Compost Evaluation in Oats, Pepper and Eggplant Cultivation, *Dynamic Soil, Dynamic Plant 2 (Special Issue 1)*, **2008**, 103-109.

APPENDIX A - ICP-MS ANALYSIS RESULTS

Isotope	Concentration (ppm) of sample 1	Concentration (ppm) of sample 2	Concentration (ppm) of sample 3	Average Concentration (ppm)
Al 27	5492.43	8484.27	6070.96	6682.55
V 51	14.99	36.81	15.44	22.41
Cr 52	57.72	102.30	61.76	73.92
Mn 55	448.07	683.87	469.36	533.77
Fe 57	41658.22	63870.54	44750.00	50092.92
Co 59	8.39	25.46	7.83	13.89
Ni 61	30.89	78.14	46.61	51.88
Cu 63	504.76	781.26	524.47	603.50
Zn 66	960.28	1473.66	1048.83	1160.92
As 75	9.98	26.04	9.89	15.30
Cd 111	8.27	25.08	7.63	13.66
Pb 208	101.15	166.03	104.87	124.02

APPENDIX B - ZETA POTENTIAL MEASUREMENTS RESULTS

I (mol/L)	Sample 1		Sample 2		Sample 3		Average	
	pH	ζ (mV)	pH	ζ (mV)	pH	ζ (mV)	pH	ζ (mV)
0.001M	2.00	7.55	1.87	7.95	2.04	7.88	1.97	7.79
	3.00	-1.97	3.47	-9.03	2.91	-2.53	3.13	-4.51
	3.11	-3.28	4.00	-8.46	3.34	-5.88	3.48	-5.87
	4.35	-11.7	5.42	-21.40	6.32	-28.60	5.36	-20.57
	6.47	-31.4	6.31	-27.20	8.01	-23.60	6.93	-27.40
	8.26	-21.4	7.55	-25.80	9.10	-28.70	8.30	-25.30
	10.09	-30.8	9.40	-27.70	-	-	6.50	-19.50
0.01M	2.05	7.25	1.94	6.88	2.00	7.24	2.00	7.12
	2.94	-1.39	3.00	-3.28	2.99	-1.68	2.98	-2.12
	4.00	-13.1	3.99	-13.40	4.01	-12.90	4.00	-13.13
	5.05	-19.3	4.91	-20.80	4.90	-20.50	4.95	-20.20
	6.23	-29.4	6.35	-30.30	6.69	-27.50	6.42	-29.07
	7.00	-25.6	7.00	-23.20	7.89	-26.20	7.30	-25.00
	8.00	-24.5	8.00	-26.50	8.11	-27.40	8.04	-26.13
0.1M	9.80	-29.80	9.10	-27.90	9.04	-30.90	9.31	-29.53
	2.03	4.15	1.89	5.26	2.06	6.31	1.99	5.24
	3.05	-3.14	3.02	-4.57	2.99	-2.47	3.02	-3.39
	4.03	-9.72	4.10	-8.92	4.05	-10.25	4.06	-9.63
	5.00	-15.10	4.97	-17.63	5.28	-19.54	5.08	-17.42
	6.45	-18.60	6.56	-19.24	6.58	-19.70	6.53	-19.18
	7.05	-18.10	7.01	-19.59	7.08	-23.48	7.05	-20.39
7.87	-19.60	7.94	-20.04	7.99	-25.62	7.93	-21.75	
9.56	-20.00	9.14	-26.34	9.26	-27.18	9.32	-24.51	

APPENDIX C – SURFACE MODIFICATION TRIALS RESULTS

Polyelectrolyte	Dose (mg polyelectrolyte/ mg solids)	Zeta potential (mV)	Polyelectrolyte	Dose (mg polyelectrolyte/ mg solids)	Zeta potential (mV)	
PEI	0	-29.1	PDADMAC	0	-23.9	
	0.002	-24		0.002496	-19.6	
	0.004	-14.55		0.004992	-20.3	
	0.006	-5.48		0.007488	-14.2	
	0.008	0.35		0.009984	-13.3	
	0.01	0.87		0.01248	-6.28	
	0.012	2.4		0.014976	-4.09	
	0.014	6.53		0.017472	-3.79	
PAM	0	-23		0.02496	-3	
	0.001	-14.5		0.027456	-2.49	
	0.002	-7.9		0.029952	0.769	
	0.003	-4.85		0.032448	2.85	
	0.004	-2.23		0.034944	4.14	
	0.005	0.012		0.03744	9.47	
	0.006	2.71		PEO	0	-29
	0.008	4.05			0.001	-21.2
	0.009	4.23	0.002		-29.7	
PAA	0	-18.2	0.003		-19.3	
	0.001	-17.1	0.004		-18.2	
	0.002	-18.4	0.005	-19.9		
	0.003	-18.5	0.006	-20		
	0.004	-19	0.007	-22.3		
	0.006	-19.9	0.009	-19.3		
			0.02	-19.4		
			0.05	-21.8		
			0.07	-20.2		

APPENDIX D – PARTICLE SIZES CHANGES WITH AMENDMENTS RESULTS

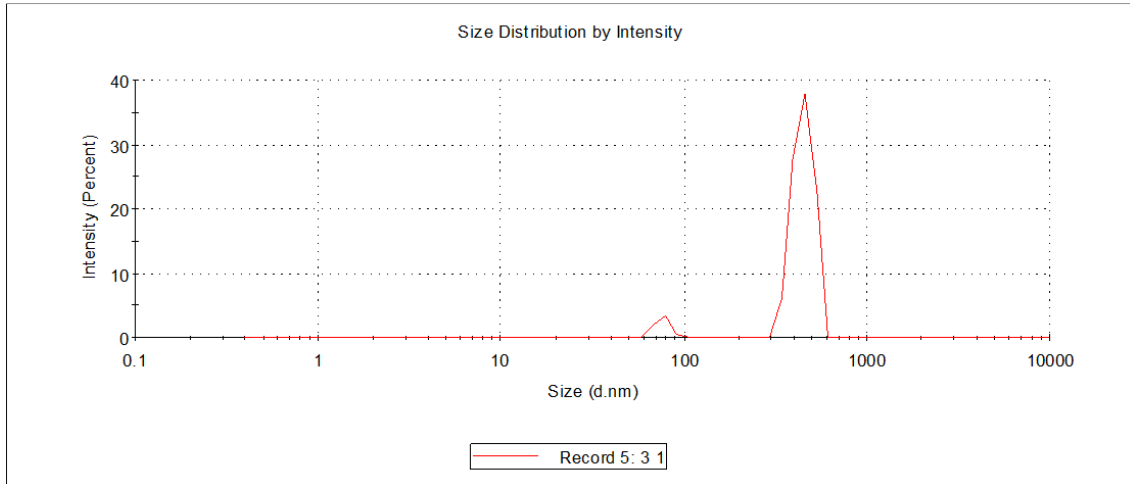


Fig. 1 Selected Biosolids Size Distribution without Particle Size Amendments

Temperature (°C): 20.0	Duration Used (s): 50
Count Rate (kcps): 54.6	Measurement Position (mm): 4.65
Cell Description: Disposable sizing cuvette	Attenuator: 7

	Size (d.nm):	% Intensity:	St Dev (d.nm):
Z-Average (d.nm): 2592	Peak 1: 342.0	100.0	6.607e-6
PdI: 1.000	Peak 2: 0.000	0.0	0.000
Intercept: 1.22	Peak 3: 0.000	0.0	0.000
Result quality : Refer to quality report			

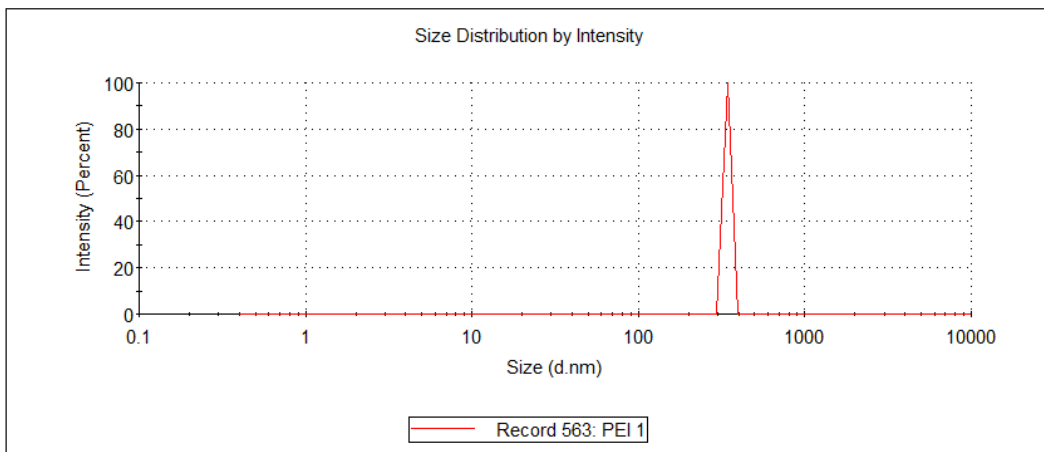


Fig. 2 Particle Size Amendment with optimal dose of PEI

Temperature (°C): 20.0	Duration Used (s): 50
Count Rate (kcps): 5.9	Measurement Position (mm): 1.25
Cell Description: Disposable sizing cuvette	Attenuator: 6

	Size (d.nm):	% Intensity:	St Dev (d.nm):
Z-Average (d.nm): 4964	Peak 1: 342.0	61.0	0.000
Pdl: 0.808	Peak 2: 0.7674	39.0	0.05616
Intercept: 1.24	Peak 3: 0.000	0.0	0.000

Result quality : Refer to quality report

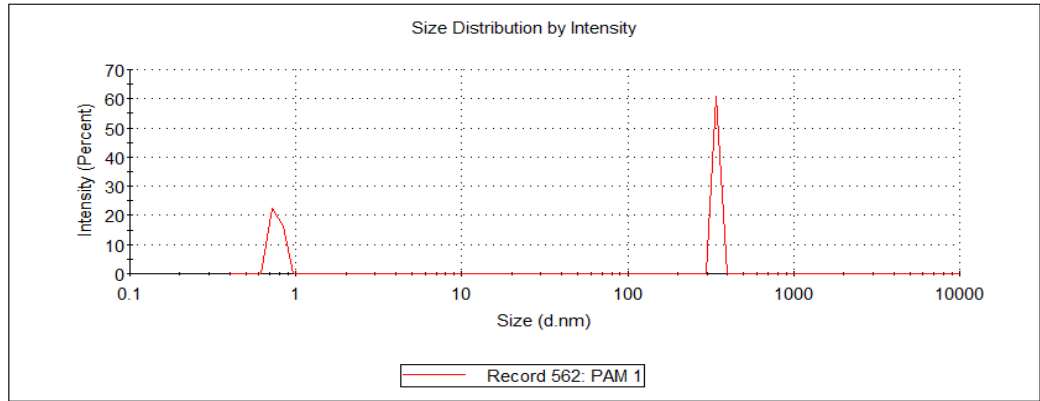


Fig. 3 Particle Size Amendment with optimal dose of PAM

	Size (d.nm):	% Intensity:	St Dev (d.nm):
Z-Average (d.nm): 4549	Peak 1: 3594	89.8	658.0
Pdl: 0.353	Peak 2: 180.0	10.2	15.11
Intercept: 0.948	Peak 3: 0.000	0.0	0.000

Result quality : Refer to quality report

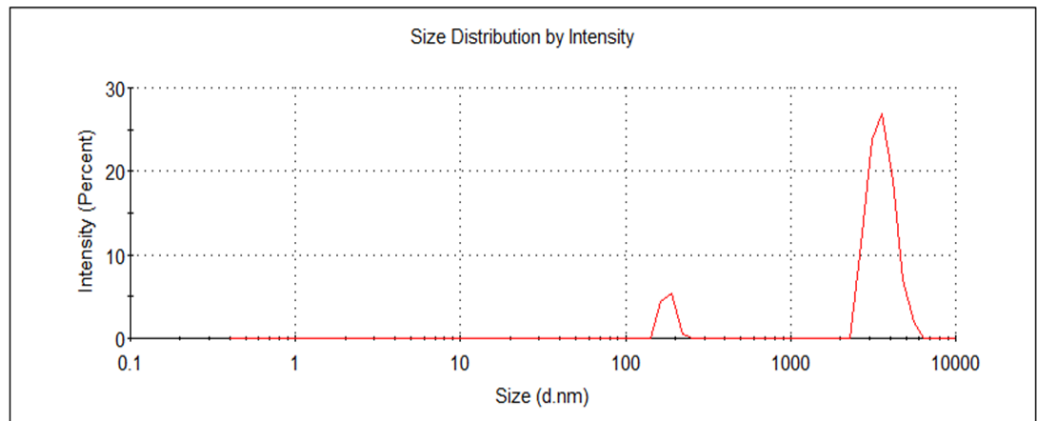


Fig. 4 Particle Size Amendment with optimal dose of PDADMAC

APPENDIX E- AFM ANALYSIS RESULTS

